# pH and Redox-Responsive Pickering Emulsions Based on Cellulose Nanocrystal Surfactants

Yang Yang,[+][a] Huilou Sun,[+][a] Meng Wang,[b] Mingwei Li,[a] Zhen Zhang,[c] Thomas P. Russell,*[d,e] Shaowei Shi*[a]

[a] Y. Yang, H. Sun, M. Li, Prof. S. Shi
Beijing Advanced Innovation Center for Soft Matter Science and Engineering & Beijing Engineering Research Center for the Synthesis and Applications of Waterborne Polymers, Beijing University of Chemical Technology, Beijing 100029, China
E-mail: shisw@mail.buct.edu.cn

[b] M. Wang
Beijing Xinfeng Aerospace Equipment Co., Ltd, Beijing 100854, China

[c] Prof. Z. Zhang
SCNU-TUE Joint Lab of Device Integrated Responsive Materials (DIRM), South China Academy of Advanced Optoelectronics, South China Normal University, Guangzhou 510006, People's Republic of China

[d] Prof. T. P. Russell
Department of Polymer Science and Engineering, University of Massachusetts, Amherst, Massachusetts 01003, USA
E-mail: russell@mail.pse.umass.edu

[e] Prof. T. P. Russell
Materials Sciences Division, Lawrence Berkeley National Laboratory, 1 Cyclotron Road, Berkeley, California 94720, USA

[+] These authors contributed equally to this work.

Supporting information for this article is given via a link at the end of the document.

**Abstract:** Nanoparticle surfactants (NPSs), formed by using dynamic interactions between nanoparticles and complementary ligands at the liquid-liquid interface, have emerged as "smart emulsifiers" with attributes of high emulsification efficiency, long-term stability, and on-demand emulsification/demulsification capabilities. However, only pH-responsiveness can be adopted to the assembly of reported NPSs formed by electrostatic interactions. Here, we propose an alternative design strategy, by taking advantage of the ferrocenium ($Fc^+$)-sulphate ion pair, to develop a new type of cellulose nanocrystal (CNC) surfactant. The $Fc^+$ groups are sensitive to pH, redox reagents and voltage, imparting the CNC surfactants and derived Pickering emulsions with multi-stimuli-responsiveness, showing promising applications in controllable delivery, release, and biphasic biocatalysis.

Pickering emulsions are dispersions of immiscible liquids, where the interfaces are stabilized by colloidal particles.[1] The dense packing and high binding energy of the particles to the interface afford a strong mechanical barrier against the coalescence of droplets,[2] offering the Pickering emulsions a superior stability that is attractive in many commercial products and industrial processes[3]. Recent advances in some biphasic applications, such as heterogeneous catalysis and molecular delivery, require an on-demand emulsification/demulsification in response to external stimuli, promoting the development of dynamically stable Pickering emulsions.[4] The manipulation of the formation, breakage, and switching of such emulsions has led to the development of "smart emulsifiers", whose interfacial activity and adsorption state can be reversibly transformed by various triggers.[5]

The energy associated with the binding of particles to liquid-liquid interfaces is dominated by the size of particles and the wettability of particle surfaces, where the latter is reflected in the three-phase contact angle.[6] In comparison to typical colloiidal particles, the small size of nanoparticles (NPs) gives rise to a low binding energy at the liquid-liquid interface and a dynamic adsorption/desorption behavior,[7] limiting their emulsification efficiency. Modifying the wettability of particle surface providea an alternative strategy to enhance the interfacial activity of NPs but usually requires multiple synthetic steps or time-consuming processes. Nanoparticle surfactants (NPSs), an emergent class of interfacially active materials, have overcome this impediment and have attracted increasing interest in the past decade.[8] By using interactions between NPs dispersed in one liquid and polymer/oligomer ligands with complementary functionality dissolved in a second immiscible liquid, multiple ligands anchor to the NPs at the interface to maximize the reduction in the interfacial energy per NP, forming "Janus-like" NPSs *in situ* at the interface, where the binding energy of each NP to the interface is significantly increased. NPSs form and assemble at the interface, stabilizing the interface, and, when compressing the interface, NPSs jam, affording the possibility to lock liquids in non-equilibrium shapes.[9] With NPSs, stable Pickering emulsions of different types (o/w, w/o and o/w/o) and droplet sizes (from several tens to hundreds of microns) can be easily obtained.[10] Notably, the formation of NPSs is driven by non-covalent interactions, such as electrostatic, host-guest, and charge-transfer interactions.[11] These dynamic interactions impart the NPSs with an adaptive assembly/disassembly ability in response to pH, light, redox, or guest-competitive triggers, affording a smart control of the emulsification/demulsification processes, that has shown potential applications in many fields including encapsulation, delivery and controlled release.[12] To date, NPSs formed by electrostatic interactions are generally based on ion pairs, e.g., ammonium-carboxylate, where only pH-responsiveness can be achieved to manipulate the assemblies.[11a,13] Many biphasic uses of Pickering emulsions are sensitive to the additives or accumulated products generated during the emulsification/demulsification processes,[14] making current stimuli strategies unsuitable. Consequently, alternative designs for NPS-based Pickering emulsions with multiple-stimuli responsiveness, and new phase-switching strategies that are convenient, mild, and repeatable, are needed.

Here, we report a new type of smart NPSs, cellulose nanocrystal (CNC) surfactants, that form by the electrostatic interactions between sulphated cellulose nanocrystals (CNC-$OSO_3^-$) and ferrocenium terminated polystyrene (PS-$Fc^+$) at the oil-water interface (Scheme 1). The $Fc^+$ groups are sensitive to redox reagents,[15] voltage,[14b,16] and pH,[17] offering multiple

routes to manipulate the interactions between the $Fc^+$-$OSO_3^-$ ion pair, and the consequent assembly/disassembly of the CNC surfactants. When used as emulsifiers, CNC surfactants have a high emulsification efficiency, resulting in Pickering emulsions with a long-term stability that are responsive to multiple stimuli. In particular, the electrochemical stimulus that is easy to realize, repeatable, and is, also, biocompatible, represents an ideal switching strategy that enables the use of CNC surfactants for Pickering-assisted enzymatic biocatalysis applications.

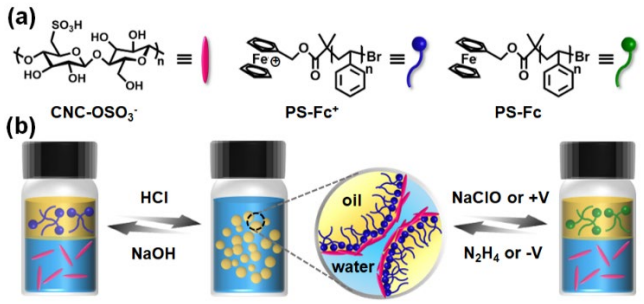


**Scheme 1.** (a) Chemical structures of CNC-$OSO_3^-$, PS-$Fc^+$, and PS-Fc. (b) Schematics of switchable emulsification/demulsification of Pickering emulsions stabilized by CNC surfactants triggered by pH, redox reagent, and voltage.

The water dispersible CNC-$OSO_3^-$ used in this work was prepared by sulfuric acid hydrolysis of CNCs. Ferrocene terminated polystyrene (PS-Fc, $M_n$ = 3.2 K, PDI = 1.1, Scheme S1 and Figures S1-S3) was dissolved in toluene and oxidized by sodium hypochlorite (NaClO, 40 mg $mL^{-1}$) *via* an electron transfer reaction.[15,16,18] The resultant PS-$Fc^+$-containing toluene solution was used as the oil phase. The interfacial activity of CNC-$OSO_3^-$ and PS-$Fc^+$ at different pH was investigated firstly, using HCl (1.0 mM) and NaOH (1.0 mM) solutions to vary the pH of aqueous phase. The time evolution of interfacial tension of the biphasic system was tracked by pendant drop tensiometry. Figure S4 shows that, in the pH range of 3.0-10, the equilibrium interfacial tensions of the biphasic systems containing CNC-$OSO_3^-$ are 33-35 mN $m^{-1}$, close to that of the pure water-toluene system (36 mN $m^{-1}$), indicating the interfacial inactivity of CNC-$OSO_3^-$.[13] In contrast, the interfacial activity of PS-$Fc^+$ is significantly affected by pH. When PS-$Fc^+$ dissolved in toluene against water with a pH of 3.0, the interfacial tension decreases to 23 mN $m^{-1}$ over 1200 s (Figure 1a-b), reflecting the surfactant-like behavior of PS-$Fc^+$. However, with the addition of NaOH, a reduced interfacial activity of PS-$Fc^+$ is seen, as evidenced by the increase of the equilibrium interfacial tension. This pH-dependent interfacial activity of PS-$Fc^+$ is similar to that seen with amine functionalized ligands, such as amine-terminated polystyrene and amine-functionalized polyhedral oligomeric silsesquioxane.[10c,13,19] Under acidic conditions, the amine group is protonated, giving these ligands an amphiphilic character and a proclivity to assemble at the interface, reducing the interfacial tension. With the addition of base, deprotonation occurs, leading to an enhanced hydrophobicity and a suppression of interfacial activity. In above two cases with only CNC-$OSO_3^-$ dispersed in water or with only PS-$Fc^+$ dissolved in toluene, when liquid is withdrawn from the droplet after equilibration, no wrinkling behavior is observed as the interfacial area decreases (Video S1), indicating that the interfacial assemblies are liquid-like in nature, and the binding energies of CNC-$OSO_3^-$ and PS-$Fc^+$ to the interface are small.

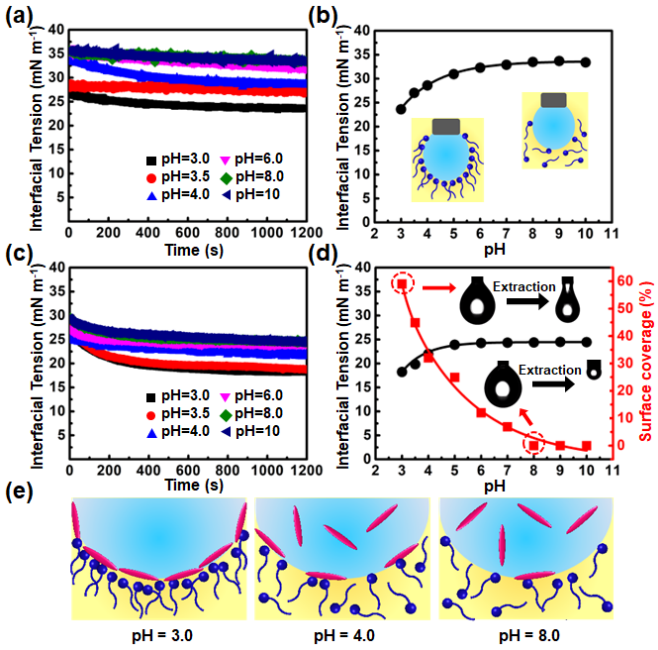


**Figure 1.** (a) Time evolution of interfacial tension and (b) equilibrium interfacial tension between PS-$Fc^+$-containing toluene solution and pure water at different pH. (c) Time evolution of interfacial tension between PS-$Fc^+$-containing toluene solution and CNC-$OSO_3^-$-containing aqueous solution at different pH. (d) Equilibrium interfacial tension between PS-$Fc^+$-containing toluene solution and CNC-$OSO_3^-$-containing aqueous solution and surface coverage of CNC surfactant at different pH. (e) Schematics of the formation of CNC surfactants at the oil-water interface at different pH. [CNC-$OSO_3^-$] = 10 mg $mL^{-1}$, [PS-$Fc^+$] = 10 mg $mL^{-1}$.

The cooperative assembly of CNC-$OSO_3^-$ and PS-$Fc^+$ is reflected in the time-dependent interfacial tension. As shown in the Figure 1c, with PS-$Fc^+$ in toluene and CNC-$OSO_3^-$ in water at pH of 3.0, the interfacial tension rapidly decreases to 18 mN $m^{-1}$, much lower than that for systems containing only CNC-$OSO_3^-$ or PS-$Fc^+$, indicating the formation of CNC surfactants. When compressing the interface after allowing 1200 s for assembly, wrinkles are observed on the droplet surface with an apparent surface coverage of 60% (Figure 1d and Video S2) that do not relax after 30 min, indicating that the binding energies of CNC surfactants to the interface are large enough to hold the jammed assemblies to against the compression. Since the formation of CNC surfactants is dictated by the electrostatic interaction between -$Fc^+$ and -$OSO_3^-$, the pH-dependent interfacial activity of PS-$Fc^+$ endows the CNC surfactants with pH responsiveness. With the addition of NaOH, the suppressed interfacial activity of PS-$Fc^+$ weakens the electrostatic interactions (Figure 1e). As a result, the equilibrium interfacial tension increases with increasing pH (Figure 1d), while the apparent surface coverage decreases, with no interfacial jamming occurring above a pH of 8.0 (Figure 1d and Video S3). Furthermore, the interfacial activity and jamming of CNC surfactants can be finely controlled by varying the concentration of either CNC-$OSO_3^-$ or PS-$Fc^+$ (Figure S5 and S6). Using oscillatory pendant drop tensiometry, the rheological properties of CNC surfactant-based interfacial assemblies were investigated. As shown in Figure S7, over the frequency range from 0.01 to 1.0 Hz, both the viscous ($E''(\omega)$) and elastic ($E'(\omega)$) components of the modulus are obtained, with the elastic part dominating, demonstrating the elastic nature of the interfacial

assemblies. 2D macroscopic films assembled by dense packing of CNC surfactants at the interface are evidenced by transmission electron microscopy (TEM), where the images show a robust co-assembly of CNC-$OSO_3^-$ and PS-$Fc^+$ (Figure S8). Water contact angle measurements on films transferred to silicon wafers yielded values of ~102° (hydrophobic) and ~40° (hydrophilic) for the different sides of the film, refecting its Janus nature (Figure S9).

By reducing $Fc^+$ group to Fc group, the redox-responsiveness of CNC surfactants can be achieved. As shown in Figure 2a, with CNC-$OSO_3^-$ dispersed in water and reduced PS-Fc dissolved in toluene (PS-Fc is obtained by adding the reductant, hydrazine hydrate ($N_2H_4$), to the PS-$Fc^+$-containing toluene solution), the equilibrium interfacial tension is 26 mN $m^{-1}$, much higher than that of CNC surfactants (18 mN $m^{-1}$), but close to that with only PS-Fc dissolved in toluene (27 mN $m^{-1}$, Figure S10). When compressing the interface, wrinkles are observed at large compression, accompanied with a rapid relaxation (Figure 2b and Video S4). These results indicate the disassociation/disassembly of CNC surfactants, further evidencing that the formation of CNC surfactants is based on the ion pairing of $Fc^+$-$OSO_3^-$. By adjusting the amount of oxidant and reductant, the extent of oxidation and reduction of $Fc^+$ can be precisely controlled, giving tunable interfacial activity of CNC surfactants, as shown by the equilibrium interfacial tension and surface coverage in Figure 2c-d and Figure S11.

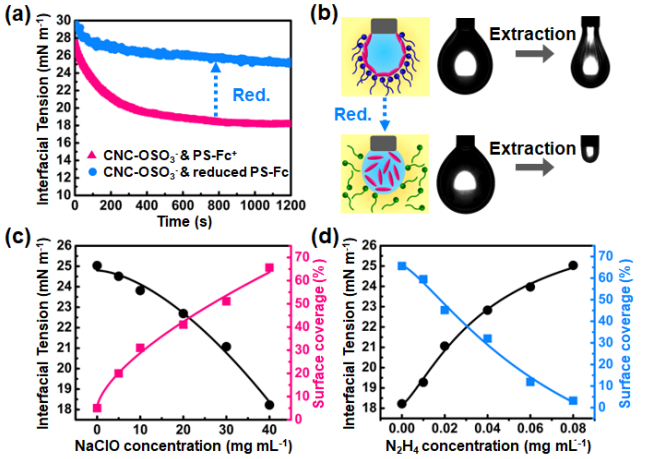


**Figure 2.** (a) Time evolution of interfacial tension in a reduction process. (b) Morphology evolution of pendent droplet in a compression process with CNC-$OSO_3^-$ in water and with PS-$Fc^+$ (up) or PS-Fc (bottom) in toluene. (c-d) Equilibrium interfacial tension and surface coverage as a function of NaClO and $N_2H_4$ concentration. [CNC-$OSO_3^-$] = 10 mg $mL^{-1}$, [PS-Fc] = 10 mg $mL^{-1}$, [PS-$Fc^+$] = 10 mg $mL^{-1}$, pH = 3.0.

Oil-in-water (o/w) Pickering emulsions were prepared by vigorously stirring a mixture of a CNC-$OSO_3^-$ aqueous dispersion and a PS-$Fc^+$ toluene solution at an oil/water ratio of 1:8, where the pH of the water phase was adjusted to 3.0. Nile Red was added to the oil phase to visualize the emulsion droplets by fluorescence microscopy. The emulsions have a long-term stability that can be retained for more than two weeks (Figure S12), indicating the irreversible anchoring of CNC surfactants to the surface of dispersed emulsion droplets that prevents coalescence. The droplet size is tunable from several tens to hundreds of microns by varying the oil/water ratio or the concentration of CNC-$OSO_3^-$ or PS-$Fc^+$ (Figures S13-S15), which reflects the superior performance of CNC surfactants as emulsifiers.

Since the CNC surfactants are responsive to pH and redox, it is necessary to determine these effects on the emulsion properties, in terms of stability and droplet size. We initiate the impact of pH. At a pH of 3.0, the emulsion droplets are stable and homogeneous with an average diameter of 57 μm (Figure 3a). An increase in the droplet size was observed with increasing pH, due to a decrease in the formation of CNC surfactants. At a pH of 9.0, the Pickering emulsion was not stable. The characteristics of the emulsions can also be adjusted by introducing a reductant. With the addition of $N_2H_4$, $Fc^+$ is reduced to Fc, causing a disassociation of CNC surfactants. The emulsion droplets enlarge gradually as the amount of reductant increases and, coalesce when the concentration of $N_2H_4$ reaches to 0.06 mg $mL^{-1}$ (Figure 3b). Moreover, since the reduction of $Fc^+$ can be triggered by electrochemical stimulation,[14b,16] voltage sensitive CNC surfactants and emulsions can be achieved. The voltage responsiveness of the emulsion was performed by using three electrodes systems. Figure 3c illustrates that the emulsion droplet size increases to over a hundred micrometers after applying a reductant voltage of -3.0 V for 10 min. By further increasing the reduction time, uniform droplets disappear and coalesce into giant droplets. A lower voltage of -1.0 V can also be used for triggering the demulsification process but it shows lower efficiency (Figure S16).[16a]

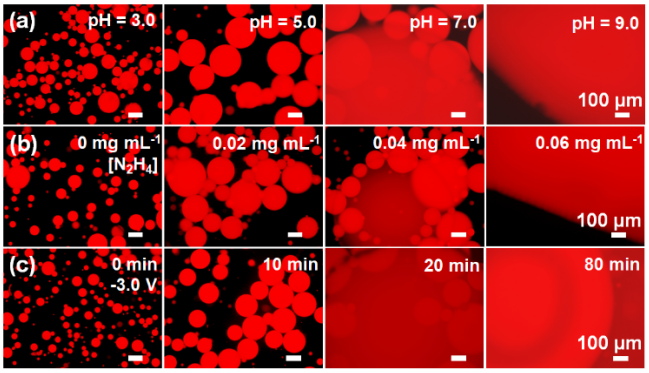


**Figure 3.** Fluorescence microscopy images showing the coalescence of o/w Pickering emulsions by (a) increasing the pH of aqueous phase; (b) adding $N_2H_4$ into the emulsion system; (c) applying a voltage of -3.0 V. $V_o$:$V_w$ =1:8, [CNC-$OSO_3^-$] = 10 mg $mL^{-1}$, [PS-$Fc^+$] = 10 mg $mL^{-1}$, [Nile Red] = 0.5 mg $mL^{-1}$, stirring rate = 1500 rpm, stirring time = 10 min.

Emulsions stabilized by CNC surfactants can, therefore, be switched between stable and unstable states in response to pH, redox reagent, and voltage triggers. As shown in Figure 4a, the pH of the water phase was set to 9.0 to promote rapid demulsification, whereas the re-emulsification requires a pH of 3.0. A coalescence and re-dispersion of emulsion droplets, accompanied with cargo release and re-encapsulation, can, therefore, be realized. Figure 4b and 4c show that this on-demand emulsification/demulsification can also be manipulated by alternatively adding $N_2H_4$ reductant and NaClO oxidant, or by applying voltages of -3.0 V and +3.0 V for 20 min. In brief, multi-stimuli-responsive Pickering emulsions based on CNC surfactants have been developed, providing versatile approaches for delivery and release applications. As far as we know, this is the first case that using electrochemical stimulation to engineer

the interfacial assembly of NPSs and NPS-based Pickering emulsions.

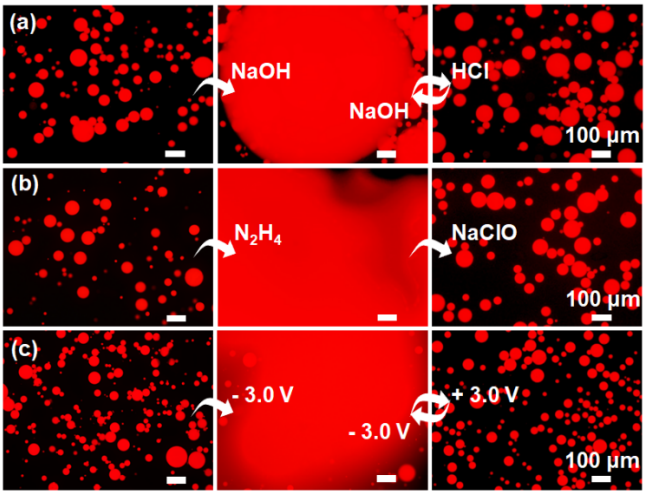


**Figure 4.** Fluorescence microscope images of the emulsification/demulsification processes of o/w Pickering emulsions triggered by (a) pH, (b) redox reagents, and (c) voltage. $V_o$:$V_w$ = 1:8, [CNC-$OSO_3^-$] = 10 mg $mL^{-1}$, [PS-$Fc^+$] = 10 mg $mL^{-1}$, [Nile Red] = 0.5 mg $mL^{-1}$.

It should be noted that, when using redox reagents as the trigger, due to the massive accumulation of salt produced in the redox process, CNCs in the continuous phase flocculate, limiting the switching to only one cycle. As for pH stimuli, since only a trace amount of NaOH and HCl solutions is required for pH adjusting, the NaCl produced is not sufficient to cause flocculation of the CNCs within three cycles, thus, the reformed emulsion is stable with no obvious change in droplet size (Figure S17). However, more cycles will cause a deterioration in the emulsion stability. In contrast, the voltage-triggered demulsification/re-emulsification can be repeated multiple times without any flocculation or cargo release, due to the absence of salt formation (Figure S18). This simple, noninvasive, and repeatable switching allows the Pickering emulsions to be used for biocatalysis applications.

Pickering emulsions have emerged as vehicles to conduct enzyme-involved biphasic biocatalysis reactions.[3c,4a,14b,20] Such emulsion systems enable catalytic reactions on the oil-dissolved substrates and water-dispersed enzymes. The solid barriers on the surface of the emulsion droplets, formed by the colloidal particles, inhibit the direct exposure of enzymes to organic solvents, protecting the enzymatic activity. Along with the enlarged interfacial area derived from the numerous droplets, a considerable catalytic efficiency can be obtained. CNC surfactant-based Pickering emulsions are a promising platform for this Pickering-assisted enzymatic biocatalysis (PAEB) application, due to (1) the use of biocompatible CNC nanoparticles,[21] (2) the high catalysis efficiency arising from the large interfacial area, and (3) a re-usability given by the mild electrochemical stimulation.

A representative hydrolysis reaction of olive oil was performed to evaluate the PAEB performance of the CNC surfactant-based emulsion system. The overall design is shown in Figure 5a. The emulsion biocatalysis system was built by stirring a mixture of an aqueous solution containing CNC-$OSO_3^-$ and lipase from Candida rugose (CRL), and a toluene solution containing PS-Fc and substrate of olive oil, at an oil/water ratio of 1:8 and under an oxidation voltage of +3.0 V. The pH of the water phase was adjusted to 3.0 to ensure the assembly of CNC surfactants. After the reaction, the Pickering emulsions were demulsified, triggered by a reduction voltage of -3.0 V, to obtain the oil phase. The PS-Fc was separated by precipitating in methanol and the oleic acid product was collected after solvent evaporation. A conventional biphasic system was constructed for comparison, where the biocatalysis reaction performs in equal conditions but absent CNC surfactants.

As shown in Figure 5b and Figure S19, the hydrolysis conversion conducted in Pickering emulsion progresses over time and reaches to a conversion efficiency of 96% at 5.0 h. Further, to demonstrate the crucial role of interfacial area on the catalysis efficiency, the size of the emulsion droplet was varied. Figure S13 shows that the diameter of emulsion droplets increases by enlarging the volume fraction of oil. As a result, the interfacial areas reduce, limiting the accessibility of enzymes and suppressing the catalytic reaction (Figure 5c and Figure S20). An on-demand product separation and re-emulsification was achieved by applying a voltage of -3.0 and +3.0 V, respectively, giving the system a cyclic biocatalytic ability. Figure 5d and Figure S21 show that the conversion efficiency of the reaction, after five cycles, is still much higher than that in the first cycle of biphasic systems (34%, Figure S22). The apparent loss in efficiency after each cycle is caused by the shear-sensitivity of enzyme.[14b,22] However, it may be possible to address this issue by selecting NPs that can encapsulate the enzyme within their inner cavity,[23] then forming NPSs with PS-$Fc^+$ ligands to conduct the Pickering interfacial biocatalysis.

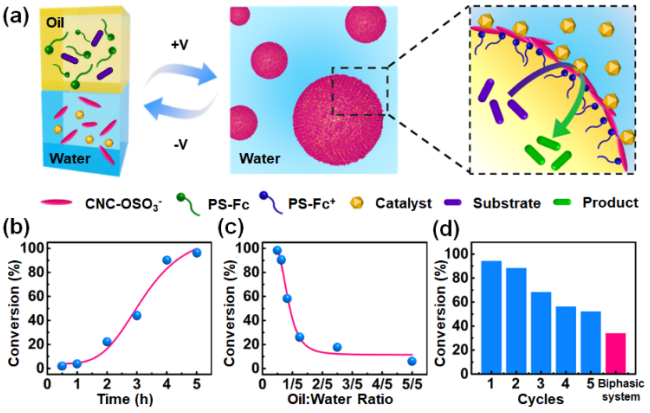


**Figure 5.** (a) Schematics of the voltage-responsive o/w Pickering emulsion for recyclable PAEB application. (b) Hydrolysis conversion efficiency of olive oil to oleic acid as a function of time. $V_o$:$V_w$ = 1:8. (c) The size effect of Pickering emulsion on the hydrolysis conversion efficiency. Reaction time = 4.0 h. (d) Re-usability in 5 cycles. $V_o$:$V_w$ = 1:8, reaction time = 4.0 h. pH = 3.0, [CNC-$OSO_3^-$] = 10 mg $mL^{-1}$, [PS-Fc] = 10 mg $mL^{-1}$, [CRL] = 10 mg $mL^{-1}$.

In summary, we have demonstrated the pH and redox-responsive Pickering emulsions stabilized by CNC surfactants. The CNC surfactants form by electrostatic interactions between CNC-$OSO_3^-$ and PS-$Fc^+$ at the oil-water interface. The precise control in tuning the electrostatic interactions enables the switching of interfacial assembly/disassembly of CNC surfactants, imparting their emulsions with a switchable emulsification/demulsification capability for encapsulation/release applications. A novel electrochemical responsiveness is

demonstrated for an NPS system, affording a simple, noninvasive, and repeatable route to control emulsions, enabling a PAEB application with high catalysis efficiency and re-usability. The co-assembly concept described offers unique opportunities to integrate functional NPs into the liquid-liquid interface, opening an avenue for Pickering interfacial catalysis applications.

## Acknowledgements

This work was supported by the National Natural Science Foundation of China (52173018, 51903011) and Beijing Natural Science Foundation (2222071). TPR was supported by the U.S. Department of Energy, Office of Science, Office of Basic Energy Sciences, Materials Sciences and Engineering Division under Contract No. DE-AC02-05-CH11231 within the Adaptive Interfacial Assemblies Towards Structuring Liquids program (KCTR16).

**Keywords:** nanoparticle surfactants • interfacial assembly • Pickering emulsions • multi-stimuli-responsiveness • biocatalysis

[1] a) R. W., *Proc. R. Soc. London* **1904**, *72*, 156-164; b) S. U. Pickering, *J. Chem. Soc., Trans.* **1907**, *91*, 2001-2021; c) B. P. Binks, T. S. Horozov, Colloidal Particles at Liquid Interfaces, Cambridge University Press, Cambridge, 2006; d) Y. Chevalier, M.-A. Bolzinger, *Colloids and Surfaces A: Physicochem. Eng. Aspects* **2013**, *439*, 23-34; e) R. Aveyard, B. P. Binks, J. H. Clint, *Adv. Colloid Interface Sci.* **2003**, *100-102*, 503-546.

[2] B. P. Binks, J. H. Clint, *Langmuir* **2002**, *18*, 1270-1273.

[3] a) C. C. Berton-Carabin, K. Schroën, *Annu. Rev. Food Sci. Technol.* **2015**, *6*, 263-297; b) H. Jiang, Y. Sheng, T. Ngai, *Curr. Opin. Colloid Interface Sci.* **2020**, *49*, 1-15; c) L. Ni, C. Yu, Q. Wei, D. Liu, J. Qiu, *Angew. Chem. Int. Ed.* **2022**, *61*, e202115885; *Angew. Chem.* **2022**, *134*, e202115885; d) Y. Yang, Z. Fang, X. Chen, W. Zhang, Y. Xie, Y. Chen, Z. Liu, W. Yuan, *Front. Pharmacol.* **2017**, *8*, 287.

[4] a) M. Pera-Titus, L. Leclercq, J. M. Clacens, F. De Campo, V. Nardello-Rataj, *Angew. Chem. Int. Ed.* **2015**, *54*, 2006-2021; *Angew. Chem.* **2015**, *127*, 2028-2044; b) J. Jiang, S. Yu, W. Zhang, H. Zhang, Z. Cui, W. Xia, B. P. Binks, *Angew. Chem. Int. Ed.* **2021**, *60*, 11793-11798; *Angew. Chem.* **2021**, *133*, 11899-11904.

[5] a) Q. Zhang, R. X. Bai, T. Guo, T. Meng, *ACS Appl. Mater. Interfaces* **2015**, *7*, 18240-18246; b) Sonia Melle, Mauricio Lask, G. G. Fuller, *Langmuir* **2005**, *21*, 2158-2162; c) B. P. Binks, R. Murakami, S. P. Armes, S. Fujii, *Angew. Chem. Int. Ed.* **2005**, *44*, 4795-4798; *Angew. Chemie.* **2005**, *117*, 4873-4876; d) J. Jiang, Y. Zhu, Z. Cui, B. P. Binks, *Angew. Chem. Int. Ed.* **2013**, *52*, 12373-12376; *Angew. Chem.* **2013**, *125*, 12599-12602; e) J. Es Sayed, C. Lorthioir, P. Banet, P. Perrin, N. Sanson, *Angew. Chem. Int. Ed.* **2020**, *59*, 7042-7048; *Angew. Chem.* **2020**, *132*, 7108-7114; f) J. Es Sayed, C. Meyer, N. Sanson, P. Perrin, *ACS Macro Lett.* **2020**, *9*, 1040-1045; g) Q. Prasser, D. Steinbach, D. Kodura, V. Schildknecht, K. König, C. Weber, E. Brendler, C. Vogt, U. Peuker, C. Barner-Kowollik, F. Mertens, F. H. Schacher, A. S. Goldmann, F. A. Plamper, *Langmuir* **2021**, *37*, 1073-1081.

[6] a) P. Pieranski, *Phys. Rev. Lett.* **1980**, *45*, 569-572; b) B. P. Binks, S. O. Lumsdon, *Langmuir* **2000**, *16*, 8622-8631; c) B. P. Binks, J. H. Clint, *Langmuir* **2002**, *18*, 1270-1273.

[7] a) B. P. Binks, *Curr. Opin. Colloid Interface Sci.* **2002**, *7*, 21-41; b) S. Shi, T. P. Russell, *Adv. Mater.* **2018**, *30*, 1800714.

[8] a) M. Cui, T. Emrick, T. P. Russell, *Science* **2013**, *342*, 460-463; b) S. Sun, T. Liu, S. Shi, T. P. Russell, *Colloid Polym. Sci.* **2021**, *299*, 523-536.

[9] a) S. Shi, X. Liu, Y. Li, X. Wu, D. Wang, J. Forth, T. P. Russell, *Adv. Mater.* **2018**, *30*, 1705800; b) J. Forth, X. Liu, J. Hasnain, A. Toor, K. Miszta, S. Shi, P. L. Geissler, T. Emrick, B. A. Helms, T. P. Russell, *Adv. Mater.* **2018**, *30*, 1707603; c) X. Liu, N. Kent, A. Ceballos, R. Streubel, Y. Jiang, Y. Chai, P. Y. Kim, J. Forth, F. Hellman, S. Shi, D. Wang, B. A. Helms, P. D. Ashby, P. Fischer, T. P. Russell, *Science* **2019**, *365*, 264–267; d) L. Li, H. Sun, M. Li, Y. Yang, T. P. Russell, S. Shi, *Angew. Chem. Int. Ed.* **2021**, *60*, 17394-17397; *Angew. Chem.* **2021**, *133*, 17534-17537; e) Y. Yang, Z. Xia, Y. Luo, Z. Wu, S. Shi, T. P. Russell, *Supramolecular Materials* **2022**, *1*, 100013.

[10] a) Y. Li, X. Liu, Z. Zhang, S. Zhao, G. Tian, J. Zheng, D. Wang, S. Shi, T. P. Russell, *Angew. Chem. Int. Ed.* **2018**, *57*, 13560-13564; *Angew. Chem.* **2018**, *130*, 13748-13752; b) S. Shi, B. Qian, X. Wu, H. Sun, H. Wang, H.-B. Zhang, Z.-Z. Yu, T. P. Russell, *Angew. Chem. Int. Ed.* **2019**, *58*, 18171-18176; *Angew. Chem.* **2019**, *131*, 18339-18344; c) B. Wang, T. Liu, H. Chen, B. Yin, Z. Zhang, T. P. Russell, S. Shi, *Angew. Chem. Int. Ed.* **2021**, *60*, 19626-19630; *Angew. Chem.* **2021**, *133*, 19778-19782; d) S. Sun, Y. Luo, Y. Yang, J. Chen, S. Li, Z. Wu, S. Shi, *Small*, **2022**, *18*, 2204182.

[11] a) C. Huang, Z. Sun, M. Cui, F. Liu, B. A. Helms, T. P. Russell, *Adv. Mater.* **2016**, *28*, 6612-6618; b) H. Sun, L. Li, T. P. Russell, S. Shi, *J. Am. Chem. Soc.* **2020**, *142*, 8591-8595; c) S. Sun, C. Xie, J. Chen, Y. Yang, H. Li, T. P. Russell, S. Shi, *Angew. Chem. Int. Ed.* **2021**, *60*, 26363-26367; *Angew. Chem.* **2021**, *133*, 26567-26571.

[12] a) H. Sun, M. Li, L. Li, T. Liu, Y. Luo, T. P. Russell, S. Shi, *J. Am. Chem. Soc.* **2021**, *143*, 3719-3722; b) B. Wang, B. Yin, Z. Zhang, Y. Yin, Y. Yang, H. Wang, T. P. Russell, S. Shi, *Angew. Chem. Int. Ed.* **2022**, *61*, e202114936; *Angew. Chem.* **2022**, *134*, e202114936; c) Z. Xia, C. G. Lin, Y. Yang, Y. Wang, Z. Wu, Y. F. Song, T. P. Russell, S. Shi, *Angew. Chem. Int. Ed.* **2022**, *61*, e202203741; *Angew. Chem.* **2022**, *134*, e202203741; d) Y. Luo, Y. Yang, Y. Wang, Z. Wu, T. P. Russell, S. Shi, *Angew. Chem. Int. Ed.* **2022**, *61*, e202207199; *Angew. Chem.* **2022**, *134*, e202207199.

[13] X. Liu, S. Shi, Y. Li, J. Forth, D. Wang, T. P. Russell, *Angew. Chem. Int. Ed.* **2017**, *56*, 12594-12598; *Angew. Chem.* **2017**, *129*, 12768-12772.

[14] a) H. Kim, S. M. Jeong, J. W. Park, *J. Am. Chem. Soc.* **2011**, *133*, 5206-5209; b) L. Peng, A. Feng, S. Liu, M. Huo, T. Fang, K. Wang, Y. Wei, X. Wang, J. Yuan, *ACS Appl. Mater. Interfaces* **2016**, *8*, 29203-29207.

[15] a) M. Nakahata, Y. Takashima, H. Yamaguchi, A. Harada, *Nat. Commun.* **2011**, *2*, 511; b) Q. Yan, A. Feng, H. Zhang, Y. Yin, J. Yuan, *Polym. Chem.* **2013**, *4*, 1216-1220.

[16] a) Qiang Yan, Jinying Yuan, Zhinan Cai, Yan Xin, Yan Kang, Y. Yin, *J. Am. Chem. Soc.* **2010**, *132*, 9268–9270; b) L. Peng, A. Feng, H. Zhang, H. Wang, C. Jian, B. Liu, W. Gao, J. Yuan, *Polym. Chem.* **2014**, *5*, 1751-1759.

[17] S. Wang, D. Du, *Sensors and Actuators B* **2004**, *97*, 373-378.

[18] Y. Liu, H. Zhang, W. Zhang, B. P. Binks, Z. Cui, J. Jiang, *Angew. Chem. Int. Ed.* **2023**, *62*, e202210050; *Angew. Chem.* **2023**, *135*, e202210050.

[19] a) G. Cerichelli, G. Illuminati, G. Ortaggi, A. M. Giuliani, *J. Organomet. Chem.* **1977**, *127*, 357-370; b) T. E. Bitterwolf, A. C. Ling, *J. Organomet. Chem.* **1972**, *40*, C29-C32.

[20] a) C. Wu, S. Bai, M. B. Ansorge-Schumacher, D. Wang, *Adv. Mater.* **2011**, *23*, 5694-5699; b) Z. Chen, L. Zhou, W. Bing, Z. Zhang, Z. Li, J. Ren, X. Qu, *J. Am. Chem. Soc.* **2014**, *136*, 7498-7504; c) Y. Wang, Q. Zhao, R. Haag, C. Wu, *Angew. Chem. Int. Ed.* **2022**, *61*, e202213974; *Angew. Chem.* **2022**, *134*, e202213974.

[21] a) Y. Habibi, L. A. Lucia, O. J. Rojas, *Chem. Rev.* **2010**, *110*, 3479-3500; b) D. Klemm, B. Heublein, H. P. Fink, A. Bohn, *Angew. Chem. Int. Ed.* **2005**, *44*, 3358-3593; *Angew. Chem.* **2005**, *117*, 3422-3458.

[22] S. Wiese, A. C. Spiess, W. Richtering, *Angew. Chem. Int. Ed.* **2013**, *52*, 576-579; *Angew. Chem.* **2013**, *125*, 604-607.

[23] a) H. Jiang, X. Hu, Y. Li, C. Yang, T. Ngai, *Chem. Sci.* **2021**, *12*, 12463-12467; b) J. Liu, G. Lan, J. Peng, Y. Li, C. Li, Q. Yang, *Chem. Commun.* **2013**, *49*, 9558-9560.

## Entry for the Table of Contents

Insert graphic for Table of Contents here.

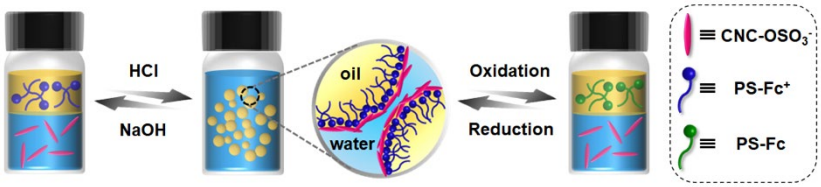


Using electrostatic interactions between sulphated cellulose nanocrystals (CNC-$OSO_3^-$) and ferrocenium terminated polystyrene (PS-$Fc^+$) at the oil-water interface, a new type of smart surfactant, termed CNC surfactants, is presented. With CNC surfactants serving as emulsifiers, pH and redox responsive Pickering emulsions are achieved, showing promising applications in encapsulation, biocatalysis, and micro-reactions.